Biomass and Bioenergy 159 (2022) 106387

Contents lists available at ScienceDirect

Biomass and Bioenergy

journal homepage: www.elsevier.com/locate/biombioe

Activated carbon from hydrolysis lignin: Effect of activation method on carbon properties

Davide Bergna [a,b,*], Toni Varila [a,b], Henrik Romar [a], Ulla Lassi [a,b]

[a] Research Unit of Sustainable Chemistry, University of Oulu, P.O. Box 3000, FI-90014, Oulu, Finland
[b] Unit of Applied Chemistry, University of Jyvaskyla, Kokkola University Consortium Chydenius, Talonpojankatu 2B, FI-67100, Kokkola, Finland

ARTICLE INFO

Keywords:
Acid pretreatment
Hydrolysis lignin
Activated carbon
Physical activation
Surface area

ABSTRACT

This study presents the effects of different activation methods to produce activated carbon from the hydrolysis lignin. Pretreatment of the feedstock with common mineral acids (HCL, HNO_3, and H_3PO_4), different steam rates for physical activation, and different chemical activating agents ($ZnCl_2$, Na_2CO_3, and KOH) for chemical activation were investigated. The pretreated biomass was carbonized and activated in one-stage process and the surface characteristics, such as total pore volume, pore size distribution and specific surface area, were investigated. The results showed that the activated carbon surface properties were not greatly affected by acid pretreatment. Brunauer-Emmett-Teller (BET) surface areas as high as 616 m^2/g could be achieved with physical activation and 2054 m^2/g with chemical activation. Different steam rates in the selected interval (0.5–2 cm^3/min) did not change the pore size distribution but had small positive effect on the specific surface area, while chemical activation with $ZnCl_2$ increased the mesoporosity, and activation with KOH increased the microporosity and oxygen groups in the form of ether and alcohol bonds.

1. Introduction

Lignin is, next to cellulose, the second most abundant macromolecule on the earth. Typically, lignin is found in the middle lamella or cell walls [1] of wood structures, and depending on wood type, its content can vary from 15% to 25%. In the Kraft pulping process, lignin is removed in the cellulose extraction by treating wooden biomass with chemicals, typically NaOH and Na_2S with water at elevated temperatures [2]. Another process that produces lignin is the hydrolysis where biomass is treated chemically with H_2SO_4 in order to separate lignin, cellulose and hemicellulose [3]. Soda, lignosulfonate and organosolv lignin are other industrial methods to separate lignin from the lignocellulose biomass while new processes like steam explosion (SE) lignin and ammonia fiber expansion (AFEX) lignin are under development [4]. Lignin from the Kraft process is known as Kraft lignin and the lignin from the hydrolysis process is known as hydrolysis lignin. The major part of the lignin is produced as Kraft lignin while the hydrolysis lignin has a small but increasing part in the production. On a global scale, about 100 million tons of lignin are produced per year [5], and the main lignin usage, for example in the pulping industry, is to burn it to produce energy for pulping boilers [6].

Sources of lignin can be diverse. The most common is wood biomass; however, products from agricultural processes and wastes have also been used [7]. Biorefinery processes are often required to separate lignin from biomass to access the sugar content in cellulose and hemicellulose to produce e.g. bioethanol [8,9]. When not used as an energy source, the lignin is extracted directly as macropolymer or undergoes a depolymerization process to obtain other valuable chemicals [10]. Different types of lignin are available in industries based on the production processes used (Fig. 1).

Products with added value, such as lignosulfonates, derived from sulphite pulping and their usage in the concrete and cement industry as plasticizers, are the most useful applications for lignin [12]. Hydrolysis lignin (HL) is a major co-product of bio-ethanol production plants, and many researchers have extensively studied its structure [13,14]. So far, the full utilization of hydrolysis lignin has remained unachieved. For example, in Russia, 10,000 tons of hydrolysis lignin are produced annually and used just as a land filler material, which is not, from the environmental viewpoint, the optimal solution for the soil [15]. Other applications such as production of activated carbon, phenols, and carbon fibers from lignin have also gained much interest in the last few years. The interest in the activated carbon production has grown

* Corresponding author. Research Unit of Sustainable Chemistry, University of Oulu, P.O. Box 3000, FI-90014, Oulu, Finland.
E-mail addresses: davide.bergna@oulu.fi (D. Bergna), toni.varila@chydenius.fi (T. Varila), henrik.romar@oulu.fi (H. Romar), ulla.lassi@oulu.fi (U. Lassi).

https://doi.org/10.1016/j.biombioe.2022.106387
Received 8 April 2021; Received in revised form 24 January 2022; Accepted 20 February 2022
Available online 24 February 2022

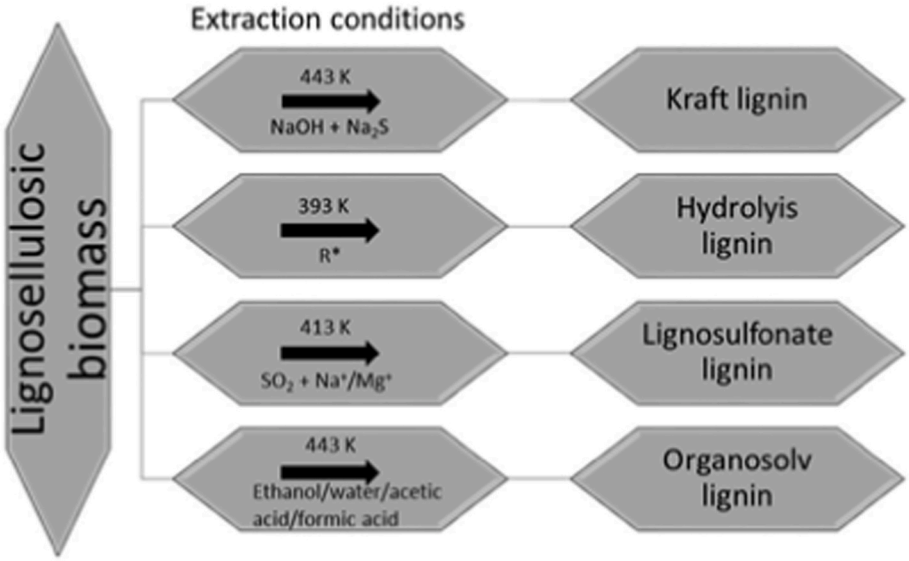

Fig. 1. Main lignin types available from lignocellulosic biomass in industrial processes [11]. R* = acid catalyzed hydrothermal pretreatment/enzymatic hydrolysis.

Table 1
Hydrolysis lignin characteristics.

Properties	Value	Unit	Standard used
Moisture	55.4	%	SFS-EN 14774-2. CEN/TS 15414-2. ISO 589
Ash (823 K)	0.2*	%	SFS-EN ISO 18122. SFS-EN 15403. ISO 1171
Volatile components	70.9*	%	SFS-EN ISO 18123. SFS-EN 15402. ISO 562
S	0.12*	%	ASTM D 4239 (mod). SFS-EN ISO 16994
C	61*	%	SFS-EN ISO 16948. SFS-EN 15407. ISO29541
H	6.1*	%	SFS-EN ISO 16948. SFS-EN 15407. ISO29541
N	0.69*	%	SFS-EN ISO 16948. SFS-EN 15407. ISO29541
O	31.9*	%	SFS-EN ISO 16993

(* on a dry basis).

significantly in Finland, mainly because the properties of activated carbon can be tailored for many applications and it can be produced from bio-based material, such as different lignin types. Kraft lignin has been proven to be a good source for producing activated carbons using chemical activation methods [16]. In the chemical activation, lignin is impregnated with activating chemicals such as KOH, NaOH, $ZnCl_2$, K_2CO_3, or H_3PO_4. The impregnated lignin is dried, sometimes milled, carbonized, and activated in an inert atmosphere at temperatures ranging from 773 K to 1073 K. In the physical activation, the lignin is carbonized and activated by steam or CO_2 in temperatures ranging from 973 K to 1073 K. Carbonization and activation performed without any pretreatments of the raw material can, in some cases, be problematic from the final application viewpoint. For example, specific types of activated carbon used in medical care or in the cosmetic industry should have certain purity levels, such as low ash and metal contents, to use safely (e.g., Ph Eur CAS 7440-44-0). The action of the acids appears to benefit dehydration reactions by removing OH-groups as water, leaving porous structures richer in carbon content. The pretreatment with a weak organic acid (acetic acid) modified the pore size distribution in activated carbons, most likely due to the removal of easy leaving groups [17].

To utilize hydrolysis lignin, this study focuses on the production of activated carbon from hydrolysis lignin with physical and chemical activation methods. Physical activation was performed using three different steam rates at the same activation temperature (1073 K), while the chemical activation was performed using three different chemical activation agents ($ZnCl_2$, Na_2CO_3, and KOH) at three different temperatures (773 K, 873 K and 1073 K). Properties such as specific surface area (SSA), pore volume (PV), pore size distribution (PSD), yield, and total carbon (TC) content, along with elemental analysis, ICP-OES, Fourier transform infrared (FTIR) and X-ray photoelectron spectroscopy (XPS) of the activated carbon, are considered. This study gives novel information about the effect of different activating methods on the final product and gives further knowledge to the scientific community about activated carbon produced from hydrolysis lignin.

2. Materials and methods

2.1. Hydrolysis lignin

Hydrolysis lignin produced in a wood-based ethanol biorefinery was obtained from a Finnish company. Preceding the experiments, the hydrolysis lignin was dried in an oven at 378 K for 24 h to remove any moisture and finally milled and sieved into a fraction of $100 < x < 425$ μm in size. The hydrolysis lignin delivered had been analyzed for chemical properties by the supplier at a commercial laboratory. Methods used for the analyses and results obtained are presented in Table 1.

2.2. Acid pretreatment

Hydrolysis lignin was collected as bioethanol co-product, by sulfuric acid catalyzed steam explosion followed by enzymatic hydrolysis using low level ash content wood as feedstock. For the acid pretreatment, HNO_3 (65%) and HCl (32%) was ordered from Merck company and H_3PO_4 (85%) from VWR Chemicals. For chemical activation, technical grade (97%) $ZnCl_2$ was ordered from VWR Chemicals, KOH from Merck company and Na_2CO_3 from Alfa Aesar. Portions of the dried and milled hydrolysis lignin were treated with mineral acids (HCl, HNO_3, and H_3PO_4), all 1 M in concentration as water solutions under stirring and reflux for 3 h at the boiling point of each solution (373–376 K). The idea was to fully remove ash components and acid soluble, which might affect the physical properties of the produced activated carbons. After refluxing, the samples were filtered out and washed with distilled water until the pH of the filtrate was close to neutral. Samples were then dried overnight at 378 K in natural convection oven before carbonization and activation.

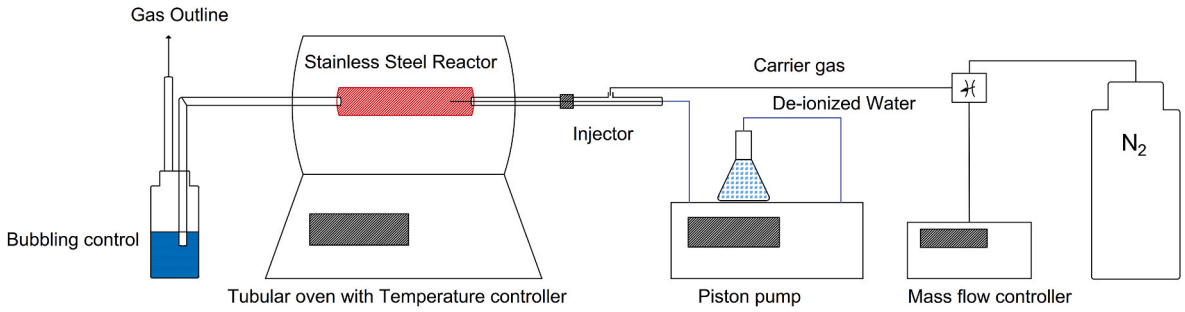

Fig. 2. Carbonization and activation setup.

Table 2
Physical activation scheme.

Sample	Temperature gradient (K/min)	Activation time (h)	Activation temperature (K)	Steam flow (g/min)	Total steam feed (g)
AC_0.5	6.5	0.5	1073	2	60
AC_1	6.5	1	1073	1	60
AC_2	6.5	2	1073	0.5	60
AC_0.5_HCl	6.5	0.5	1073	2	60
AC_1_HCl	6.5	1	1073	1	60
AC_2_HCl	6.5	2	1073	0.5	60
AC_0.5_HNO_3	6.5	0.5	1073	2	60
AC_1_HNO_3	6.5	1	1073	1	60
AC_2_HNO_3	6.5	2	1073	0.5	60
AC_0.5_H_3PO_4	6.5	0.5	1073	2	60
AC_1_H_3PO_4	6.5	1	1073	1	60
AC_2_H_3PO_4	6.5	2	1073	0.5	60

Table 3
Chemical activation scheme.

Sample	Temperature gradient (K/min)	Activation time (h)	Activation temperature (K)
KOH_T_x-y	6.5	2	873–1073
$ZnCl_2$_T_x-y	6.5	2	773–873
Na_2CO_3_T_x-y	6.5	2	1073

2.3. Carbonization and activation

After the acid pretreatment, the samples were carbonized and activated according to the setup presented in Fig. 2. A portion of about 10 g of hydrolysis lignin were placed into a stainless-steel reactor AISI 304. The physical activation with steam and the chemical activation parameters with relative sample nomenclature, are described in Table 2 and Table 3 respectively. During the activation a constant flow of 10 mL/min of nitrogen gas was assured to keep inert the atmosphere. The choice of activation temperature and heating gradient were made according to our previous experience to achieve the best possible compromise between porosity development, yield and hardware safety.

Untreated, dried, and milled hydrolysis lignin was carbonized, and steam activated in a small laboratory reactor made of stainless steel and inserted into a tubular oven. The oven was heated to the activation temperature using a temperature ramp mentioned in Table 2. At the activation temperature (1073 K), steam was injected using different holding times ranging from 0.5 to 2 h and feeds ranging from 0.5 to 2 g/min. The total volume of water, used as the activating agent, fed into the system, was the same for all the samples. Final physically activated carbons (AC) were named after the holding times and mineral acid used. For examples samples AC_1 is activated carbon produced using 1 h holding time at 1073 K with 1 g/min steam flow and AC_2_HNO_3 is activated carbon pretreated with HNO_3 followed by activation with 2 h holding time at 1073 K with 0.5 g/min steam flow.

Considering the chemically activated samples, appropriate amount of $ZnCl_2$, KOH and Na_2CO_3 was dissolved in 100–200 mL of deionized water in a 600-mL beaker. Second, the hydrolysis lignin was added to this solution to attain varying ratios of 4:1, 2:1 or 1:1 by mass (mass of activating agent/mass of hydrolysis lignin). Third, the solution was stirred using a stirring bar at 353 K for 3 h with the addition of deionized water from time to time into the solution if the water level decreased considerably. Finally, the impregnated wet hydrolysis lignin was dried in the oven at 378 K for 48 h. Then, the dried impregnated materials were placed in a stainless-steel reactor heated by a tubular oven with different temperature level selected according to the optimal "activation window" for each chemical activating agent as found in literature. Nitrogen gas was flushed through the reactor the entire time to avoid sample oxidation. After the activation, the reactor was cooled to room temperature, and the sample was collected and refluxed with a solution of 1 M HCl at 378 K for 3 h. The samples were then washed with deionized water to pH neutrality and placed in a ventilated oven to dry overnight. The final chemically activated carbon samples were named after the activating agent, temperature and ratio (chemical to feedstock mass) for example sample KOH_1073_4-1 is activated using 4/1 mass ratio of KOH at 1073 K for 2 h.

Table 4
Ashes comparison between untreated hydrolysis lignin sample and nitric acid washed hydrolysis lignin.

Sample	Al	Ca	Fe	K	Li	Mg	Na	Ni	Si	Zn	Total
	x 0.01 mg/g										
Hydrolysis lignin (untreated)	1	20	3.7	4	0.1	1.4	37.6	0.3	9	0.8	45.1
Hydrolysis lignin_HNO_3	1	20	3.0	4	0.1	0.3	0.2	0.2	9	0.7	3.9

Table 5
The effect of different steam loads on the properties of untreated and acid-pretreated activated carbons.

Sample	BET	PV cm^3/g	PSD calculated by DFT (%v/v)			TC %	Yield wt. %
	SSA m^2/g		Micro %	Meso %	Macro %		
AC_0.5	506	0.23	94	4	2	99.7	42.3
AC_1	492	0.22	95	3	2	98.2	44.4
AC_2	616	0.27	96	3	1	99.8	38.1
AC_0.5_HCl	559	0.23	93	4	3	94.4	35.2
AC_1_HCl	501	0.21	95	3	1	95.8	37.5
AC_2_HCl	589	0.23	97	3	1	96.2	25.3
AC_0.5_HNO_3	524	0.21	94	2	2	95.7	38.7
AC_1_HNO_3	504	0.22	93	5	2	97.1	40.6
AC_2_HNO_3	525	0.22	94	4	2	96.2	37.2
AC_0.5_H_3PO_4	589	0.28	85	8	7	98.9	37.5
AC_1_H_3PO_4	611	0.29	83	9	8	97.7	37.3
AC_2_H_3PO_4	561	0.24	92	6	2	95.7	38.9

2.4. Characterization of activated carbons

After physical or chemical activation, the specific surface area (SSA), pore volume (PV) and pore size distribution (PSD) of activated hydrolysis lignin samples, were determined at 77.15 K with Micromeritics 3 Flex physisorption instrument (Micromeritics Instruments, Norcross, GA, USA). Portions of each sample (100–200 mg) were degassed with Micromeritics smart VacPrep gas adsorption sample preparation device at pressure of 0.67 kPa and at a temperature of 413 K for 3 h to remove adsorbed gas. Adsorption isotherms were obtained by the immersion of the sample tubes in liquid nitrogen (77.15 K) to achieve constant temperature conditions and by the dosing of volumes of gaseous nitrogen in the samples.

Data were processed with 3Flex version 5.02 software. SSAs were calculated from adsorption isotherms according to the Brunauer–Emmett–Teller (BET) method [18]. The model selected to estimate the PSD and PV of activated carbon material was non-linear density functional theory (NLDFT) based on a model of independent slit-shaped pores specifically designed for carbon structured materials [19–22]. The pore size distribution was calculated from the individual volumes of micropores, mesopores, and macropores with the NLDFT model. By using the instrumental setup, micropores down to a diameter of 0.35 nm can be measured. A previous study has reported that SSAs are typically measured with a precision of 5% [23].

2.5. X-ray photoelectron spectroscopy

X-ray photoelectron spectroscopy analyses were performed using the Thermo Fisher Scientific ESCALAB 250Xi XPS System. The carbon samples were placed on an indium film with a pass energy of 20 eV and a spot size of 900 μm; the accuracy of the reported binding energies (BEs) was ±0.3 eV. O and C elemental data were collected for all samples. The measured data were analyzed with Avantage V5 Software. The monochromatic AlKα radiation (1486.7 eV) was operated at 20 mA and 15 kV. Charge compensation was used to determine the presented spectra, and the BE calibration was performed by applying the C1s line at 284.8 eV as a reference (531.2 eV for the O1s line).

2.6. Elemental analysis, TC, and field emission scanning electron microscopy

Elemental analysis was performed with a Flash 2000 CHNS–O organic elemental analyzer produced by Thermo Scientific. The ground sample was first weighed to 1.5–3.5 mg and dried for 1 h at 378 K. Then, the sample was placed in the analyzer and mixed with 10 mg of vanadium pentoxide V_2O_5 to enhance the burning. The prepared sample was

Table 6
Effect of chemical activation agent ratio and activation temperature on feedstock material.

Sample	BET	PV cm^3/g	PSD calculated by DFT (%v/v)			TC %	Yield wt. %
	SSA m^2/g		Micro %	Meso %	Macro %		
$ZnCl_2$_500_4-1	1742	1.36	31	69	0	86.8	6.7
$ZnCl_2$_600_4-1	1626	1.23	33	67	0	96.5	9.2
KOH_800_1-1	928	0.45	83	13	4	69.8	2.6
KOH_800_2-1	1202	0.53	91	7	2	81.6	8.9
KOH_800_4-1	2054	0.90	94	5	1	70.6	3.5
KOH_600_4-1	1099	0.51	93	6	1	58.9	7.2
Na_2CO_3_800_4-1	514	0.25	91	7	2	82.1	8.6

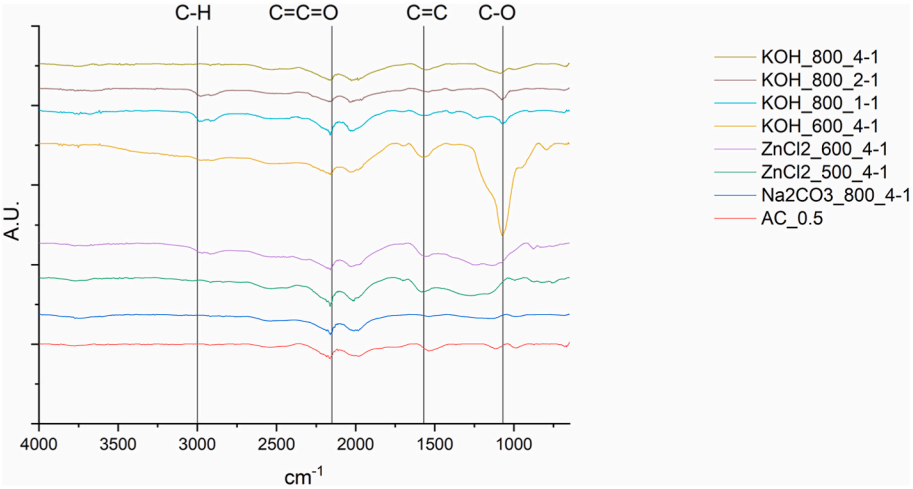

Fig. 3. FTIR analysis of physical and chemically activated hydrolysis lignin samples.

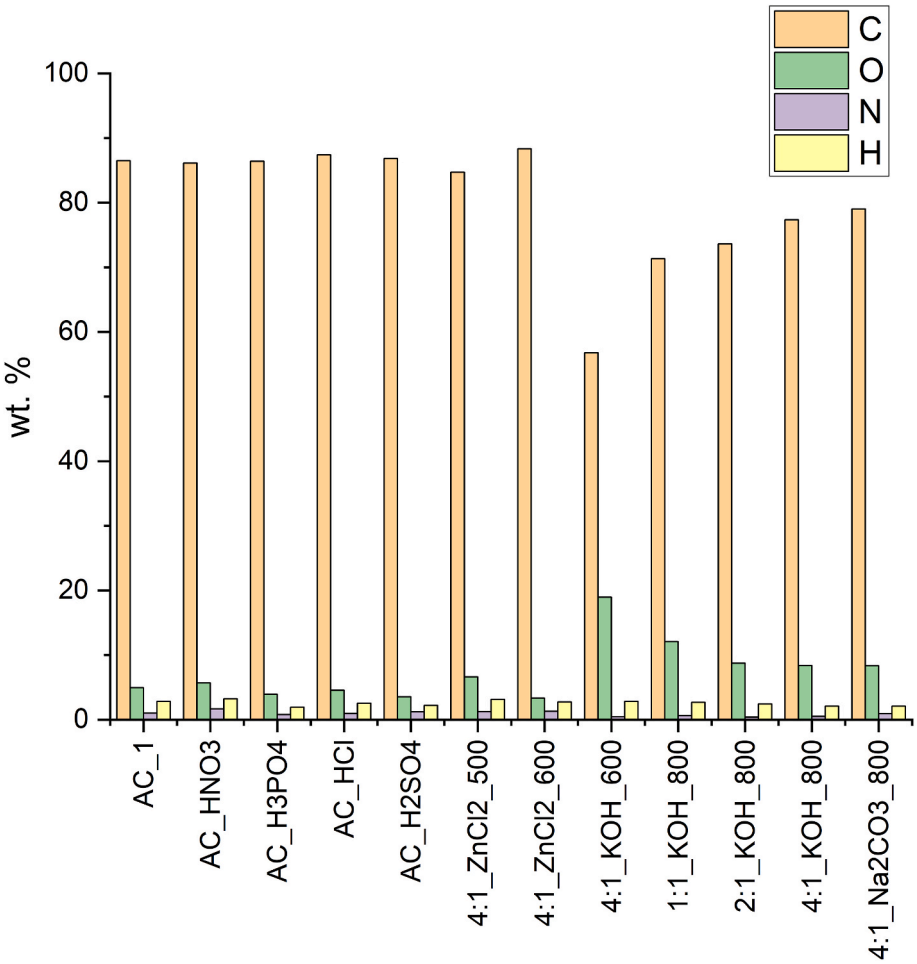

Fig. 4. Elemental analysis comparison of physical and chemical activated hydrolysis lignin samples (Sulphur was also measured and it was below the detection limit).

then combusted at a temperature of 1233 K for 600 s using a standard methionine for hydrogen and nitrogen, while the standard used for oxygen was BBOT 2,5-(Bis (5-*tert*-butyl-2-benzo-axazol-2-yl) thiophene. Plain tin cups were used as a bypass (three pcs) when starting the measurements.

TC percentage present in each sample was measured using a Skalar Primacs MCS instrument. Dried samples were weighed in quartz crucibles and then combusted at 1373 K in a pure oxygen atmosphere, after which the formed CO_2 was analyzed by an IR analyzer built in the Skalar Formacs analyzer. Carbon content values were obtained by reading the signal of the IR analyzer from a calibration curve derived from known masses of a standard substance, citric acid. The carbon content of the individual samples was calculated as a percentage of the initially weighed mass.

A field emission scanning electron microscope (FESEM) was used to study the microstructure of the sample. The FESEM images were obtained using a Zeiss Sigma field emission scanning electron microscope (Carl Zeiss Microscopy GmbH, Jena, Germany) at the Centre for Material Analysis in the University of Oulu operated at 5 kV.

2.7. Fourier transform infrared analysis

Fourier transform infrared (FTIR) spectra were obtained using an ATR–FTIR spectrometer (PerkinElmer Spectrum One) with diamond/ZnSe crystal. The scans were obtained in the spectral range of 4000–650 cm^{-1}, with a resolution of 4 cm^{-1} and 20 scans for each sample.

2.8. ICP-OES (Inductively coupled plasma optical emission spectroscopy)

For the ICP-OES measurement, PerkinElmer Optima 5300 DV instrument, was used to compare the total metal content (ashes) within the raw hydrolysis lignin and acid treated hydrolysis lignin. Samples weighing 0.1–0.2 g were first digested with 9 mL of HNO_3 at 473 K for 10 min in a microwave oven (MARS, CEM Corporation). Then, 3 mL of HCl was added, and the mixture was digested at 473 K for 10 min. Finally, 1 mL of HF was added, and the mixture was again digested at 473 K for 10 min. Excess HF was neutralized with H_3BO_3 by heating at 443 K for 10 min. Afterwards, the solution was diluted to 50 mL with water, and the elements were analyzed using the ICP-OES method. The results are reported as mg of ashes/g of sample.

3. Results and discussion

3.1. Effects of acid washing, steam feed, and holding time on the physical properties of activated carbon

The acid washing effect with three different mineral acids, HCl, HNO_3, and H_3PO_4, on the properties of activated carbons does not seem to greatly influence the final activated carbons because of the feedstock used in these experiments. Hydrolysis lignin is already washed during the recovery process and therefore, it has no vast amounts of ashes or any other acid soluble fractions that can be removed by the other mineral acids. In any case, a comparison using ICP-OES has been made comparing the most performing acid HNO_3 (Table 4), resulting in a

Table 7
XPS results for chemically activated hydrolysis lignin samples.

Sample	From C1s BE (eV)				
	C-Cconj % (284.8eV)	C-Cnon-conj % (285.0 eV)	C–O-R % (286.6 eV)	COOH (R)% (288.8 eV)	π–π* in ar. % (290.1 eV)
AC_0.5	67.49	14.25	6.84	2.08	5.14
$ZnCl_2$_500_4-1	58.47	16.26	8	3.27	5.11
$ZnCl_2$_600_4-1	59.52	19.07	7.59	3.23	5.63
KOH_800_1-1	37.7	21.0	10.0	3.5	6.5
KOH_800_2-1	52.44	6.1	7.94	3.47	6.97
KOH_800_4-1	39.23	5.05	6.81	2.55	5.72
KOH_600_4-1	28.71	5.02	6	2.89	2.41
Na_2CO_3_800_4-1	45.25	21.82	10	3.71	7.16

Sample	From O1s BE (eV)			
	C=O % (531.2 eV)	O=C/-O % (532.3 eV)	C–O % (533.8 eV)	H_2O ads. % (536.1 eV)
AC_0.5	0.97	0.95	1	0.25
$ZnCl_2$_500_4-1	1.47	2.26	3	0.56
$ZnCl_2$_600_4-1	0.88	0.94	1.12	0.32
KOH_800_1-1	3.4	5.3	10.6	1.4
KOH_800_2-1	1.42	0.82	17.58	3.09
KOH_800_4-1	4.35	0.21	28.73	3.98
KOH_600_4-1	4.8	4.48	40	4.13
Na_2CO_3_800_4-1	0.71	3.68	6	1.01

reduction mainly of Na and Mg compared to the untreated material. The total ash amount results reduced by 90%.

If acid washing were performed on another feedstock, a completely different results would be most likely obtained. For example, the effect of nitric acid treatment on the properties of the final carbons produced from palm shells increased the values of the surface characteristics of activated carbons [24].

From a scientific and industrial viewpoint, it is interesting to study the effect of steam feed injected on hydrolysis lignin at a specific time. The reaction with steam and carbon during the activation process produces carbon monoxide and hydrogen gases, which are lost from the activated sample resulting a massive weight loss but at the same time creating the porous activated carbon [25]. Usually, the steam is fed in the reactor when the activation temperature has been reached. The activation itself is then carried out within 1–6 h depending what kind of physical properties is desired from prepared activated carbons. Typically, long activation times are not a cost-friendly method from an energy consumption perspective, therefore the experiments conducted within the parameters in this study indicate that the physical properties of hydrolysis lignin depend more on the contact time than steam feed rate calculated as cm^3/min as can be seen from Table 5. One can notice a minor increase in specific surface areas and pore volume with AC_0.5, AC_1 and AC_2 samples, from 506 m^2/g to 616 m^2/g and from 0.23 cm^3/g to 0.27 cm^3/g, when contact time is increased and a small decrease in yield, 42.3 to 38.1%, as well. Other parameters were not affected by changing the contact time. Despite the small changes observed, with fast activation runs, low contact time and high steam feed, it is still possible to produce activated carbon with relatively high specific surface areas, over 500 m^2/g, with great amount of microporosity. From the industrial viewpoint, this can be a point of interest to adapt stoichiometrically the ratio to reduce the outstream condensates and obtain the same AC quality grade. The contact time considered for the experiment seems to be a factor effecting the physical properties; thus, a shorter time can be implemented to obtain AC with equivalent porous characteristics.

In Table 5 are reported the different effect on the physisorption of the produced activated carbon induced by the acid treatment. The only noticeable difference is given by the slight reduction of microporosity caused by H_3PO_4 pretreatment. Thus, the effects of the pretreatment are negligible compared with the effects caused by the steam activation on the pore developments.

3.2. *Effects of chemical activation on activated carbon physical properties*

Considering the chemical activation, the results showed that with the chemical activation agents considered for this study, a high level of SSA can be achieved, and this is particularly true for $ZnCl_2$ and KOH (Table 6). Samples activated with $ZnCl_2$, can reach up to 1740 m^2/g SSA with a great pore volume, 1.36 cm^3/g, and majority of the created pores are larger than 2 nm, which indicates mesoporous carbon structure within the samples. This result is in line with other similar biomass

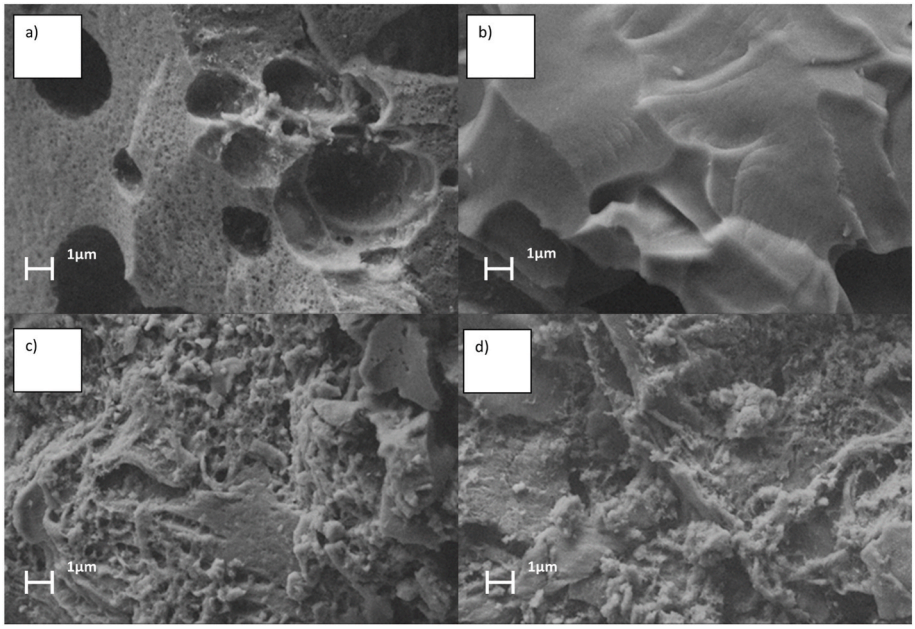

Fig. 5. FESEM images a) KOH_800_1–1, b) $ZnCl_2$_500_4-1, c) Na_2CO_3_800_4-1, d) AC_0.5.

based activated carbons activated with $ZnCl_2$ [26,27]. The reagent to carbon ratios greatly influenced the KOH activation, where at ratios 4–1, over 2000 m^2/g of SSA was obtained with pore volume of 0.90 cm^3/g. $ZnCl_2$, however, favors the production of mesopores, while KOH and Na_2CO_3 determine a higher production of microporosity. This result agrees with previous studies performed on other feedstock types, such as peat [28].

The yield results were influenced by the different chemical ratios, and it is particularly evident regarding KOH, where the increase in surface area corresponds to a decrease in yield value [29]. One explanation to low yield might be the reaction of KOH with carbon at high temperatures, which produces metallic potassium, hydrogen gas and sodium carbonate [30]. Due to the acid washing, after the chemical activation, the carbon, in sodium carbonate, will be lost as a CO_2, which explains the low yield obtained.

Regarding the TC, a lower level of carbon content was measured compared with the physical activation, especially with the KOH activated samples. These results suggested that there might still be some metallic potassium or sodium carbonate trapped inside the pores or some of the other elements were present in the sample in a quantity not compatible with the relative ash content.

3.3. *Effect of chemical activation on the activated carbon surface functional groups*

One of the most interesting observations in this study is that, with the chemical activation of hydrolysis lignin, it is possible not only to tailor the physical adsorption properties such as SSA and PSD, but also to modify the activated carbon composition, inducing a probably different type of functional groups on the activated carbon surface (Fig. 3). The graphs represent a comparison between steam-activated carbon surfaces and chemically activated carbons.

According to the combined FTIR spectra of chemically activated carbons, when finding a compromise between increasing the KOH to feedstock ratio and reducing the activation temperature, the band around 1070–1150 cm^{-1} is growing. This peak corresponds to the C–O stretching vibrations [31]. This result shows that it is possible to increase the oxygen content on the carbon surface using KOH and that the increase is higher if the temperature does not exceed 873 K. This result occurs at a price of a lower SSA compared to the 1073 K activation, but still with a reasonable value of 1099 m^2/g (Table 6). Band between 1550 and 1650 cm^{-1} belongs to C═C stretching from aromatic rings or conjugated system. Other peaks at 3000 cm^{-1} and 2200 cm^{-1} correspond to C–H and C═C═O band stretching [32]. With $ZnCl_2$ or Na_2CO_3 activation, there are no relevant differences in the FTIR spectrum compared to the AC_0.5 spectrum.

The elemental analysis of chemically activated carbons (Fig. 4) confirms that, with KOH, it is possible to increase the oxygen content of the carbons. Furthermore, chemical activation performed with Na_2CO_3 also slightly increased the oxygen content of the final carbons. However, $ZnCl_2$ activation lowered oxygen, nitrogen, and hydrogen contents of the carbons compared to AC_0.5.

The analysis with XPS in Table 7, confirms the previous characterizations evidencing that the amount of oxygen increased on the carbon KOH-activated surface is mainly in the form of a C–O bond with some presence of C═O, which is slightly higher compared to the other activated samples. In this analysis, it is also interesting to observe that the Na_2CO_3 activation, even if not determining any increase in the oxygen content, seems to slightly drift the carbonization from a C–C conjugated to a C–C nonconjugated bond system.

The FESEM qualitative analysis is presented in Fig. 5. It is possible to evidence a porous structure partially given by the lignin morphology and by the chemical activating agent.

4. Conclusions

In this study, activated carbon from hydrolysis lignin was produced. Acid pretreatment with HCl, HNO_3, and H_3PO_4, physical activation with steam and chemical activation with $ZnCl_2$, KOH, and N_2CO_3 were tested. The results showed that acid pretreatment did not substantially affect the porous characteristics of activated carbon produced from hydrolysis lignin. Acid pretreatment with nitric acid, however, decreased the total ash content of raw hydrolysis lignin material even if the material originally came from process where low pH values are needed. Both physical and chemical activation developed substantial porosity. Physical activation was performed with the same amount of total steam load but at different contact times and steam feeds. Results indicated that with longer contact times, slightly higher SSA values were obtained but as demonstrated in this study similar values can be obtained with faster activations also. From industrial viewpoint, this finding can benefit the activated carbon process economically. Chemical activation with $ZnCl_2$ determined the creation of mesoporous activated carbon, while KOH caused an increase in the oxygen groups on the mainly microporous activated carbon surface area. The properties of the activated carbons produced from hydrolysis lignin are comparable with the commercial ones, which means that potentially they can be used for the same application purposes.

Author contributions

Conceptualization HR, TV, DB; methodology: DB, TV, HR.; investigation: DB.; data curation: DB.; writing—original draft preparation: DB, TV, HR; writing—review and editing: DB, TV, HR.; supervision: UL.; project administration: UL; funding acquisition: UL. All authors have read and agreed to the published version of the manuscript."

Funding

This research was funded by European Regional Development Fund grant number A75548 Carbotech and by the Green Bioraff Solutions Project (EU/Interreg/Botnia-Atlantica, 20201508).

Declaration of competing interest

The authors declare no conflicts of interest in the results.

Acknowledgments

Authors acknowledge Sari Tuikkanen for the total carbon analysis, Hanna Prokkola for the elemental analysis, and Dr. Hu Tao for the XPS and FESEM characterization.

References

[1] R. Alén, Structure and chemical composition of wood, For. Prod. Chem. (2000) 12–57.
[2] F.S. Chakar, A.J. Ragauskas, Review of current and future softwood kraft lignin process chemistry, in: 2ndInd. Crops Prod, 20, Elsevier, 2004, pp. 131–141.
[3] D.M. de Carvalho, J.L. Colodette, Comparative study of acid hydrolysis of lignin and polysaccharides in biomasses, Bioresources 12 (4) (2017) 6907–6923, https://doi.org/10.15376/biores.12.4.6907-6923.
[4] A. Berlin, M. Balakshin, Industrial lignins: analysis, properties, and applications, in: Bioenergy Res. Adv. Appl., Elsevier, 2014, pp. 315–336.
[5] D.S. Bajwa, G. Pourhashem, A.H. Ullah, S.G. Bajwa, A concise review of current lignin production, applications, products and their environment impact, Ind. Crop. Prod. 139 (2019), https://doi.org/10.1016/j.indcrop.2019.111526.
[6] G. Gellerstedt, M. Ek, G. Henriksson, Wood Chemistry and Biotechnology, de Gruyter, 2009, p. 308.
[7] W. Li, K. Amos, M. Li, Y. Pu, S. DeBolt, A.J. Ragauskas, J. Shi, Fractionation and characterization of lignin streams from unique high-lignin content endocarp feedstocks, Biotechnol. Biofuels 11 (2018), 304, https://doi.org/10.1186/s13068-018-1305-7.
[8] Y. Liao, S.F. Koelewijn, G. van den Bossche, J. van Aelst, S. van den Bosch, T. Renders, K. Navare, T. Nicolaï, K. van Aelst, M. Maesen, H. Matsushima, J. M. Thevelein, K. van Acker, B. Lagrain, D. Verboekend, B.F. Sels, A sustainable

wood biorefinery for low-carbon footprint chemicals production, Science 367 (2020) 1385–1390, https://doi.org/10.1126/science.aau1567.
[9] D.G. Mulat, J. Dibdiakova, S.J. Horn, Microbial biogas production from hydrolysis lignin: insight into lignin structural changes, Biotechnol. Biofuels 11 (2018), 61, https://doi.org/10.1186/s13068-018-1054-7.
[10] O. Yu, K.H. Kim, Lignin to materials: a focused review on recent novel lignin applications, Appl. Sci. 10 (13) (2020), 4626, https://doi.org/10.3390/app10134626.
[11] N. Mandlekar, A. Cayla, F. Rault, S. Giraud, F. Salaün, G. Malucelli, J.-P. Guan, An overview on the use of lignin and its derivatives in fire retardant polymer systems, in: Lignin - Trends Appl., InTech Open, 2018, pp. 207–231.
[12] A.L. Macfarlane, M. Mai, J.F. Kadla, Bio-based chemicals from biorefining: lignin conversion and utilisation, in: Adv. Biorefineries Biomass Waste Supply Chain Exploit, Woodhead publishing, 2014, pp. 659–692.
[13] M.J. Zarubin, S.R. Alekseev, S.M. Krutov, Hydrolysed lignin. Structure and perspectives of transformation into low molecular products, in: Recent Adv. Environ. Compat. Polym., Woodhead publishing, 2001, pp. 155–160.
[14] J.F. Kennedy, G.O. Phillips, P.A. Williams, H. Hatakeyama, Recent Advances in Environmentally Compatible Polymers, Woodhead publishing, 2001.
[15] H. Hatakeyama, Y. Tsujimoto, M.J. Zarubin, S.M. Krutov, T. Hatakeyama, Thermal decomposition and glass transition of industrial hydrolysis lignin, in: J. Therm. Anal. Calorim, 101, Springer, 2010, pp. 289–295.
[16] Z. Yang, R. Gleisner, D.H. Mann, J. Xu, J. Jiang, J.Y. Zhu, Polymers (Basel), Lignin Based Activated Carbon Using H3PO4 Activation, 12, MDPI, 2020, 2829.
[17] D. Bergna, H. Romar, U. Lassi, C, Physical Activation of Wooden Chips and the Effect of Particle Size, Initial Humidity, and Acetic Acid Extraction on the Properties of Activated Carbons, 4, MDPI, 2018, 66.
[18] S. Brunauer, P.H. Emmett, E. Teller, Adsorption of gases in multimolecular layers, J. Am. Chem. Soc. 60 (1938) 309, https://doi.org/10.1021/ja01269a023.
[19] M. Thommes, B. Smarsly, M. Groenewolt, P.I. Ravikovitch, A. V Neimark, Adsorption hysteresis of nitrogen and argon in pore networks and characterization of novel micro- and mesoporous silicas, Langmuir 22 (2006) 756–764, https://doi.org/10.1021/la051686h.
[20] A. V Neimark, P.I. Ravikovitch, A. Vishnyakov, Bridging scales from molecular simulations to classical thermodynamics: density functional theory of capillary condensation in nanopores, J. Phys. Condens. Matter 15 (2003) 347–365, https://doi.org/10.1088/0953-8984/15/3/303.
[21] C. Lastoskie, K.E. Gubbins, N. Quirke, Pore size heterogeneity and the carbon slit pore: a density functional theory model, Langmuir 9 (1993) 2693–2702, https://doi.org/10.1021/la00034a032.
[22] J. Landers, G.Y. Gor, A. V Neimark, Density functional theory methods for characterization of porous materials, Colloids Surf. A Physicochem. Eng. Asp. 437 (2013) 3–32, https://doi.org/10.1016/j.colsurfa.2013.01.007.
[23] V.A. Hackley, A.B. Stefaniak, "Real-world" precision, bias, and between-laboratory variation for surface area measurement of a titanium dioxide nanomaterial in powder form, J. Nanoparticle Res. 15 (2013), 1742, https://doi.org/10.1007/s11051-013-1742-y.
[24] A. Allwar, R. Hartati, I. Fatimah, Effect of nitric acid treatment on activated carbon derived from oil palm shell, in: 1stAIP Conf. Proc, 1823, AIP Publishing, 2017, 020129.
[25] H.E. Klei, J. Sahagian, D.W. Sundstrom, Kinetics of the activated carbon-steam reaction, Ind. Eng. Chem. Process Des. Dev. 14 (4) (1975) 470–473, https://doi.org/10.1021/i260056a020.
[26] T. Varila, H. Brännström, P. Kilpeläinen, J. Hellström, H. Romar, J. Nurmi, U. Lassi, From Norway spruce bark to carbon foams: characterization, and applications, Bioresources 15 (2020), https://doi.org/10.15376/biores.15.2.3651-3666.
[27] T. Varila, E. Mäkelä, R. Kupila, H. Romar, T. Hu, R. Karinen, R.L. Puurunen, U. Lassi, Conversion of furfural to 2-methylfuran over CuNi catalysts supported on biobased carbon foams, Catal. Today 367 (2021) 16–27, https://doi.org/10.1016/j.cattod.2020.10.027.
[28] T. Varila, D. Bergna, R. Lahti, H. Romar, T. Hu, U. Lassi, Activated carbon production from peat using ZnCl2: characterization and applications, Bioresources 12 (2017) 8078–8092, https://doi.org/10.15376/BIORES.12.4.8078-8092.
[29] D. Bergna, T. Hu, H. Prokkola, H. Romar, U. Lassi, Effect of Some Process Parameters on the Main Properties of Activated Carbon Produced from Peat in a Lab-Scale Process 11, Waste and Biomass Valorization, 2019, pp. 2837–2848.
[30] M.A. Lillo-Ródenas, D. Cazorla-Amorós, A. Linares-Solano, Understanding chemical reactions between carbons and NaOH and KOH: an insight into the chemical activation mechanism, Carbon N. Y. 41 (2) (2003) 267–275, https://doi.org/10.1016/S0008-6223(02)00279-8.
[31] Sigma Aldrich, IR Spectrum Table & Chart | Sigma-Aldrich, IR Spectr, Table Chart., 2018.
[32] T. Hase, Tables of Organic Spectrometry, tenth ed., Otatieto, Helsinki, 2008.